

Comparing early dark energy and extra radiation solutions to the Hubble tension with BBN

Osamu Seto^{1,2,*} and Yo Toda^{2,†}

¹*Institute for the Advancement of Higher Education,*

Hokkaido University, Sapporo 060-0817, Japan

²*Department of Physics, Hokkaido University, Sapporo 060-0810, Japan*

Abstract

A shorter sound horizon scale at the recombination epoch, arising from introducing extra energy components such as extra radiation or early dark energy (EDE), is a simple approach resolving the so-called Hubble tension. We compare EDE models, an extra radiation model, and a model in which EDE and extra radiation coexist, paying attention to the fit to big bang nucleosynthesis (BBN). We find that the fit to BBN in EDE models is somewhat poorer than that in the Λ CDM model, because the increased inferred baryon asymmetry leads to a smaller deuterium abundance. We find that an extra radiation-EDE coexistence model gives the largest present Hubble parameter H_0 among the models studied. We also examine data sets dependence, whether we include BBN or not. The difference in the extra radiation model is $3.22 < N_{\text{eff}} < 3.49$ (68%) for data sets without BBN and $3.16 < N_{\text{eff}} < 3.40$ (68%) for data sets with BBN, which is so large that the 1σ border of the larger side becomes the 2σ border.

*Electronic address: seto@particle.sci.hokudai.ac.jp

†Electronic address: y-toda@particle.sci.hokudai.ac.jp

I. INTRODUCTION

The Λ CDM cosmological model has been successful in explaining the properties and evolution of our Universe. However, various low-redshift measurements of the Hubble constant H_0 have reported a significantly larger value than that inferred from the temperature anisotropy of cosmic microwave background (CMB) measured by *Planck* (2018) $H_0 = 67.36 \pm 0.54$ km/s/Mpc [1]. SH0ES measures the Hubble constant by using Cepheids and type Ia supernovae as standard candles and has reported $H_0 = 73.45 \pm 1.66$ km/s/Mpc in Ref. [2] (R18) and $H_0 = 74.03 \pm 1.42$ km/s/Mpc in Ref. [3] (R19). Similarly, the H0LiCOW Collaboration obtained the result $H_0 = 73.3 \pm 1.7$ km/s/Mpc from gravitational lensing with time delay [4]. Since all local measurements of H_0 by different methods consistently indicate a larger value of H_0 than that from *Planck*, even if there is an unknown systematic error [5–8], this discrepancy cannot be easily solved [9].

As this discrepancy seems serious, several ideas for an extension of the Λ CDM model have been proposed to solve or relax this tension. A modification in the early Universe would be more promising than our during later times, because low-redshift z cosmology is also well constrained by baryon acoustic oscillation (BAO) measurements. One approach to relax the Hubble tension is to introduce a beyond-the-standard-model component [9, 10]. One of the simplest methods is to increase the relativistic degrees of freedom parametrized by N_{eff} [1]. By quoting the value

$$N_{\text{eff}} = 3.27 \pm 0.15(68\%), \quad (1)$$

for (CMB+BAO+R18) from the *Planck* Collaboration [1], it has been regarded that $0.2 \lesssim \Delta N_{\text{eff}} \lesssim 0.5$ is preferred to relax the H_0 tension. Several beyond-the-standard-model proposals [11, 12] could accommodate such an extra N_{eff} . Some of them are interesting because they can address not only the Hubble tension, but also other subjects such as the anomalous magnetic moment of the muon [12], the origin of neutrino masses [13] or a sub-GeV weakly interacting massive particle dark matter [14]. Another popular scenario is so-called early dark energy (EDE) models, where a tentative dark energy component somewhat contributes the cosmic expansion around the recombination epoch [15–31]. The main

idea of how to relax the Hubble tension by adding an extra energy component is summarized as follows.

Once the cosmic expansion rate is enhanced by introducing a new extra component, the comoving sound horizon for acoustic waves in a baryon-photon fluid at the time of recombination with the redshift z_* becomes shorter than that in the standard Λ CDM model.

The position of the first acoustic peak in the CMB temperature anisotropy power spectrum corresponds to its angular size θ_* , which is related to the sound horizon r_{s*} by $\theta_* \equiv r_{s*}/D_{M*}$, with the angular diameter distance

$$D_{M*} = \int_0^{z_*} \frac{dz}{H(z)}. \quad (2)$$

For a fixed measured θ_* , the reduction of D_{M*} due to the shorter r_{s*} leads to a larger Hubble parameter, because the primary term of the integrand in Eq. (2) at low z does not change much.

The effects of the shorter sound horizon due to new components like those mentioned above can be seen in the power spectrum as a shift of peak positions to higher multipoles ℓ . Other effects are to let the first and second peaks higher as well as other high ℓ peaks lower. The magnitudes of the change of the peak heights and position shifts depend on the specific extra component model. On the other hand, as is well known, generally an increase of the dark matter density shifts the spectra to lower ℓ values and reduces the height of the peaks, and an increase of the baryon density extends the height difference between the first and second peaks [32]. The scalar spectral index n_s controls the spectral tilt of the whole range of the spectrum. In order to compensate the new component effects on the power spectrum, the dark matter density needs to be increased to return the original spectrum that matches with the Λ CDM, and then the baryon density also needs to be increased to adjust the relative height of the first and second peaks.

This approach is limited due to the resultant modification to the Silk damping scale, i.e., the photon diffusion scale [33]. One way to see the first problem is the fact that, as mentioned above, the phase shift and damping of the amplitude of high- ℓ peaks cannot be well recovered by changing only the dark matter and baryon density¹. For EDE models, a poor fit to large-scale structure data has also been claimed [36, 37], which can be seen in the

¹ For a scenario free from this diffusion problem, see Refs. [34, 35].

value of σ_8 in Ref. [17]. Despite this limitation, the introduction of extra radiation or EDE is a simple extension of Λ CDM that addresses the H_0 discrepancy. The extra radiation energy and EDE contribute differently throughout the whole cosmological history. While EDE significantly contributes to the energy budget only around the epoch of matter-radiation equality to recombination and its energy density decreases quickly, the extra radiation exists throughout the whole history of the Universe. This difference can be seen in its effects on big bang nucleosynthesis (BBN). In fact, a study for N_{eff} with referring BBN in the context of the Hubble tension was done in Refs. [38, 39]. In EDE models, although the negligible energy density of the EDE component at the BBN epoch appears not to change the BBN prediction, the baryon abundance inferred from the CMB would be different from that in the Λ CDM model to adjust the CMB spectrum and hence the resultant light element abundance could be affected. In this paper, by taking the fit with BBN into account, we evaluate and compare these scenarios of additional relativistic degrees of freedoms and EDE.

This paper is organized as follows. In the next section, we first describe our modeling of the extra radiation and EDE. After we describe the methods and data sets used in our analysis in Sec. III, we show the results and discuss their interpretation in Sec. IV. The last section is devoted to a summary.

II. MODELING

The expansion rate of the Universe—the Hubble parameter,—is defined as

$$H(t) = \frac{\dot{a}}{a}, \quad (3)$$

where $a(t)$ is the scale factor and a dot denotes a derivative with respect to cosmic time t . In the following, we use the scale factor a instead of time t as a “time” variable. Then, we regard the Hubble parameter as a function of a , $H(a)$ and normalize the scale factor as $a(t_0) = a_0 = 1$, with t_0 being the age of the Universe.

A. Extra radiation

One simple “solution” to the Hubble tension is to increase the effective number of neutrinos N_{eff} , which is expressed as

$$\Omega_r = \left(1 + \frac{7}{8} \left(\frac{4}{11}\right)^{4/3} N_{\text{eff}}\right) \Omega_\gamma. \quad (4)$$

Here,

$$\Omega_i = \frac{\rho_i}{3M_P^2 H^2} \Big|_{t=t_0}, \quad (5)$$

with M_P being the reduced Planck mass, are the present values of the density parameters for i species. γ and ν stand for CMB photons and neutrinos, respectively. In the following, we call this an N_{eff} model.

B. Early dark energy

In the literature, the EDE scenarios are modeled by a variety of functional forms for scalar fields, such as axion-potential-like [15–17], polynomial [18], acoustic dark energy [20], α -attractor-like [25], and others. Those properties and differences due to various potential forms have been studied in those literatures. In contrast, in this work, since our main focus is on the differences between the EDE and the extra radiation, we adopt a simple fluid picture. In order to treat time-dependent dark energy, we define the dark energy equation of state $w(a) = p_{DE}(a)/\rho_{DE}(a)$. By integrating the continuity equation

$$\dot{\rho}_{DE} + 3H\rho_{DE}(1 + w(a)) = 0, \quad (6)$$

we obtain [40]

$$\rho_{DE}(a) = \rho_{DE}(a_0) \exp \left(- \int_a^{a_0} 3(1 + w(\hat{a})) \frac{d\hat{a}}{\hat{a}} \right). \quad (7)$$

We find the cosmic expansion by solving the Friedman equation for the EDE models

$$\frac{H^2(a)}{H_0^2} = (\Omega_c + \Omega_b)a^{-3} + \Omega_r a^{-4} + \Omega_{DE}(a), \quad (8)$$

$$\Omega_{DE}(a) = \Omega_{DE}(a_0) \exp \left(- \int_a^{a_0} 3(1 + w(\hat{a})) \frac{d\hat{a}}{\hat{a}} \right). \quad (9)$$

The indices of each Ω parameter, c, b, r , and DE , stand for cold dark matter, baryons, radiation, and dark energy, respectively. Here, DE represents the sum of the EDE component

and the cosmological constant Λ which is responsible for the present accelerating cosmic expansion as $\rho_{\text{DE}}(a) = \rho_{\text{EDE}}(a) + \rho_{\Lambda}$.

In the EDE scenarios, the energy component of dark energy becomes significant around the moment of the matter-radiation equality and contributes to about several percents of the total energy density. Soon after that moment, the EDE component decreases as $\rho_{\text{DE}} \propto a^{-n}$ and faster than the background energy densities do. Here we introduce two parameters: a_c and a_m . a_c is the scale factor at the moment when the EDE starts to decrease like radiation ($n = 4$) or kination ($n = 6$). a_m is the scale factor at the moment when the EDE component becomes as small as the cosmological constant. Phenomenologically, we parametrize the equation of state $w(a)$ as

$$w_n(a) = -1 + \frac{n}{3} \frac{(a_c^n + a_m^n)a^n}{(a_c^n + a^n)(2a_c^n + a_m^n + a^n)}, \quad (10)$$

and the resultant Ω parameter is given by

$$\Omega_{\text{DE}n}(a) = \Omega_{\Lambda} \frac{a^n + 2a_c^n + a_m^n}{a^n + a_c^n}. \quad (11)$$

For $a < a_c$ and $a_m < a$, the dark energy behaves like a cosmological constant. Typical evolutions of $w_n(a)$ and $\rho_{\text{DE}n}(a)$ normalized by ρ_{Λ} are shown in Fig. 1. We note that the above $\Omega_{\text{DE}n}(a)$ is proportional to the f_{EDE} parameter often used in literature as

$$f_{\text{EDE}}(a) = \Omega_{\text{DE}n}(a) \frac{H_0^2}{H^2(a)}. \quad (12)$$

Typical evolutions of $f_{\text{EDE}}(a)$ are shown in Fig. 2.

Since Eq. (11) can be approximated as

$$\Omega_{\text{DE}n}(a)|_{a=1} \simeq \Omega_{\Lambda}(1 + a_m^n) = \Omega_{\Lambda} + \Omega_{\text{EDE}}, \quad (13)$$

we will use $\Omega_{\text{EDE}}/\Omega_{\Lambda}$ as a variable parameter instead of a_m .

Dealing perturbation, in this work we set its effective sound speed $c_s^2 = 1$ for perturbations of the EDE component, motivated by a class of scalar field models. One may compare this to each specific scalar potential model in e.g., Refs. [15–17, 19, 24, 25, 29, 30]. Our modeling will be closer to nonoscillatory scalar field models [20, 25].

III. DATA AND ANALYSIS

We perform a Markov Chain Monte Carlo (MCMC) analysis on an N_{eff} model and the EDE model described in the previous section. We use the public MCMC code

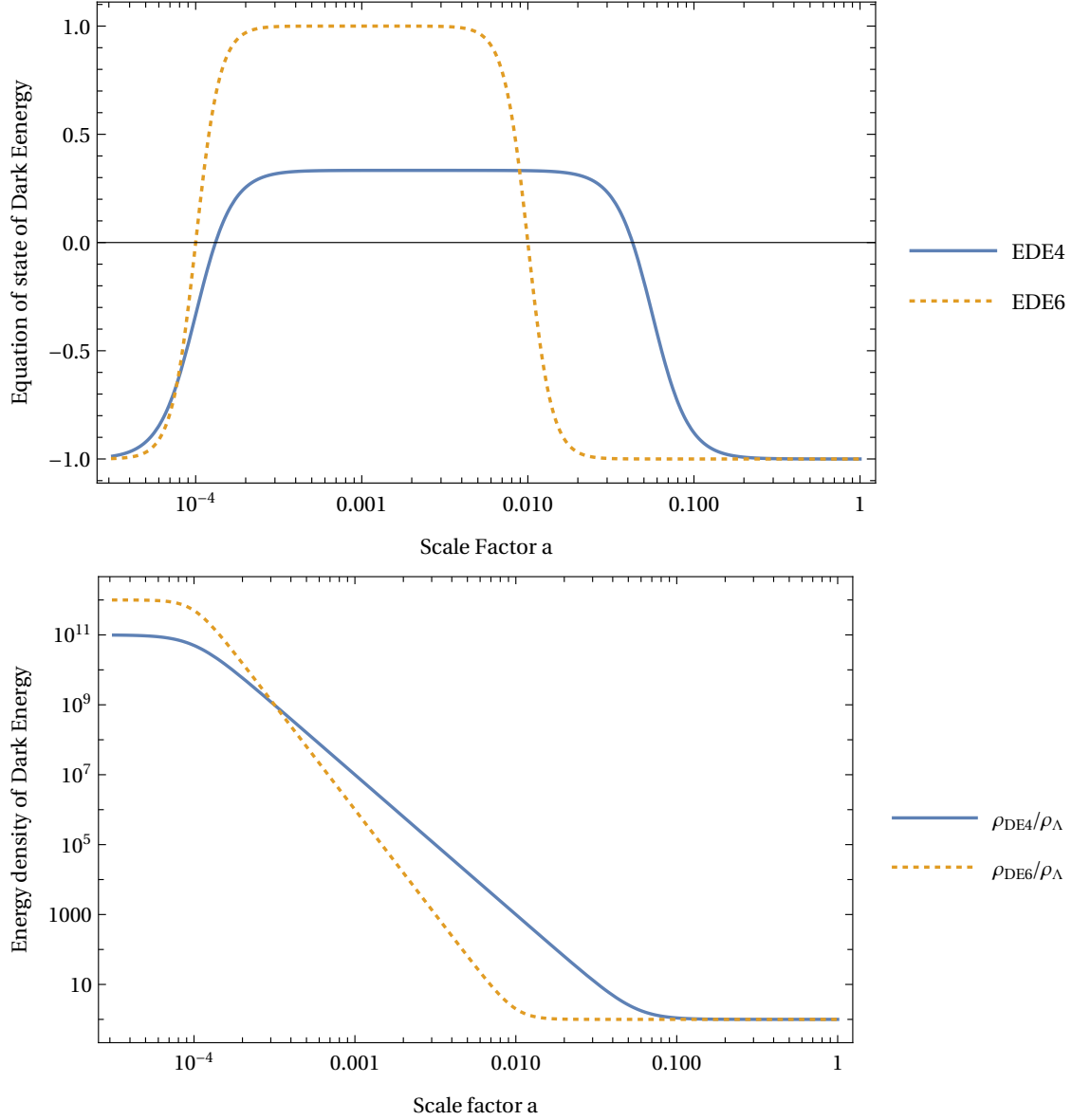


FIG. 1: Evolution of the equation-of-state parameter w_n and $\rho_{DEn}(a)/\rho_{\Lambda}$ for $n = 4$ and 6 . For definiteness, in these plots we take $a_c = 10^{-4}$, $a_m = 10^{-5/4}$ for $n = 4$ and $a_c = 10^{-4}$, $a_m = 10^{-2}$ for $n = 6$. We can confirm that ρ and w behave like radiation or kination for $a_c < a < a_m$ and like a cosmological constant for $a < a_c$ and $a_m < a$.

CosmoMC-planck2018 [41] and implement the above EDE scenarios by modifying its equation file in CAMB. For estimation of light elements, we use PArthENoPE standard [42] in CosmoMC.

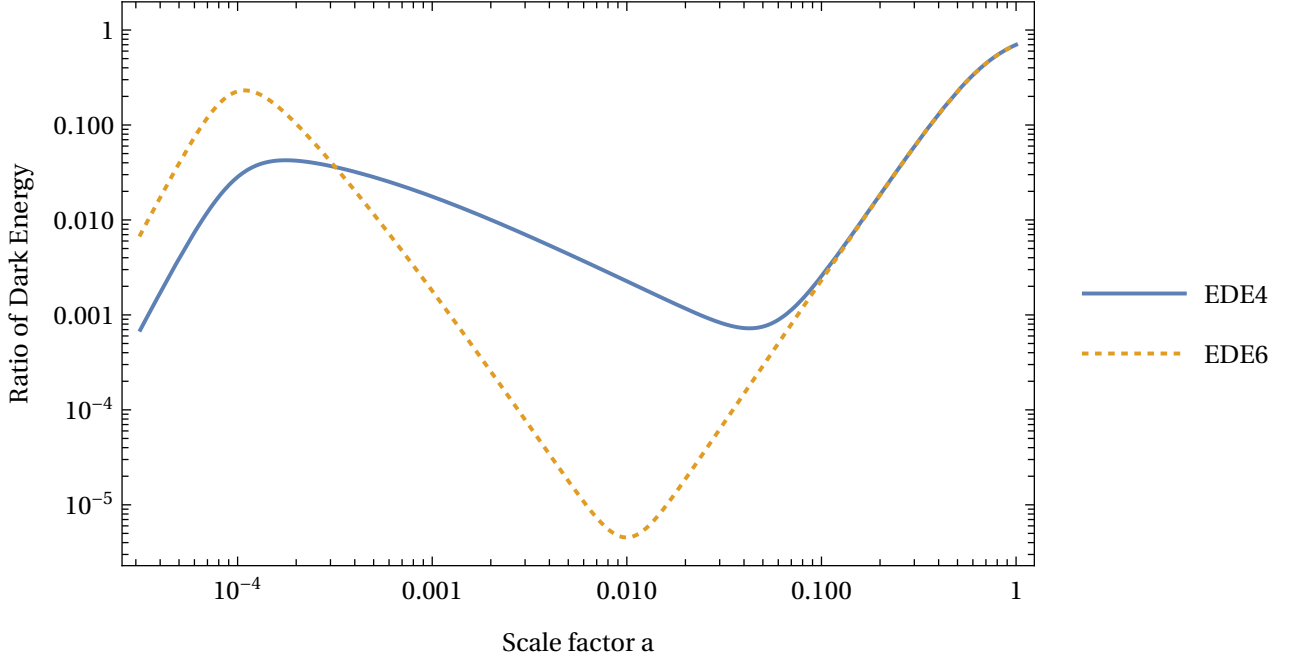


FIG. 2: Evolution of $f_{\text{EDE}}(a)$. The choices of a_c and a_m are the same as in Fig. 1.

A. Data sets

We analyze models using the following cosmological observation data sets. We include both temperature and polarization likelihoods for high l ($l = 30$ to 2508 in TT and $l = 30$ to 1997 in EE and TE) and low- l **Commander** and low- l **SimAll** ($l = 2$ to 29) of Planck (2018) measurement of the CMB temperature anisotropy [1]. We also include *Planck* lensing data [43]. For constraints on low-redshift cosmology, we include BAO data from 6dF [44], DR7 [45], and DR12 [46]. We also include Pantheon data [47] on the local measurement of light curves and luminosity distance of supernovae, as well as SH0ES (R19) data [3] on the local measurement of the Hubble constant from the Hubble Space Telescope’s observation of Supernovae and Cepheid variables. Finally, we include the data sets on the helium mass fraction Y_P [48] and deuterium abundance D/H [49] to impose the constraints from BBN.

B. EDE and neutrino parameter sets

We take a prior range of $N_{\text{eff}} \in [2.2, 3.6]$. This is motivated by the 2σ limit $2.2 \lesssim N_{\text{eff}} \lesssim 3.6$ (BBN+ Y_P +D/H, 2σ) in Ref. [50].

For the EDE model with $n = 4$, which is denoted as EDE4 hereafter, we fix $a_c = 10^{-4}$

and vary parameters in the range $\Omega_{\text{EDE}}/\Omega_{\Lambda} \in [1 \times 10^{-7}, 1 \times 10^{-5}]$. For the EDE model with $n = 6$, which is denoted as EDE6 hereafter, we fix $a_c = 3 \times 10^{-4}$ and vary parameters in the range $\Omega_{\text{EDE}}/\Omega_{\Lambda} \in [1 \times 10^{-14}, 5 \times 10^{-12}]$. These values of a_c are motivated by the results in Ref. [17].

IV. RESULT AND DISCUSSION

A. Result

Although we have examined both the EDE4 and EDE6 models, we have confirmed that the EDE6 model gives a slightly better fit than the EDE4 model, as has been pointed out in previous works. Thus, we show a posterior distribution for only the EDE6 model in Fig. 3 and the posterior distribution for an N_{eff} model in Fig. 4. In addition to the above two models which have been studied in literature, we also consider the model where both the extra radiation and EDE components exist, which hereafter we call the coexisting model or EDE6 + N_{eff} , motivated by the fact that these are in principle independent sectors.

To compare models, we show the combined plots of the EDE4, the EDE6, the coexistence model with EDE6 plus N_{eff} , and N_{eff} together with ΛCDM for reference in Fig. 5. These results are also summarized in Table I. It is clear that both the EDE6 and coexistence models prefer a larger value of H_0 than other models. We confirm that the EDE4 model shows the poorest improvement for the H_0 tension, as shown in Fig. 5.

For reference, we also show the same plot of the analysis without including Pantheon and R19 data [in other words (CMB+BAO+BBN)] in Fig. 6, because one may wonder used data sets dependence. One can confirm that the results for N_{eff} in Fig. 6 almost reproduce Fig. 35 in Ref. [1]. The constraints on EDE in Figs. 5 and 6 do not differ significantly. On the other hand, we can find sizable shifts of the posterior and the central values for N_{eff} and the coexistence model, depending on whether we include R19 data. If one pays attention to only the central values, it looks like the EDE indicates the largest value of H_0 and models with N_{eff} indicate even smaller values than ΛCDM does. However, the constraints of a certain confidence level on the N_{eff} and the coexistence models are much weaker than those for the EDE model. In addition, one should be aware of the presence of the prior dependence in Fig. 6, where the energy density of EDE is positive definite, while we allow $N_{\text{eff}} < 3.046$ for

the models with N_{eff} .

Model	EDE6	EDE6+ N_{eff}	Λ CDM	N_{eff}
$\Omega_{\text{EDE}}/\Omega_{\Lambda}$	$1.00^{+0.45}_{-0.65} \times 10^{-12}$ (8.00×10^{-13})	$0.79^{+0.27}_{-0.71} \times 10^{-12}$ (5.80×10^{-13})	Λ CDM	Λ CDM
N_{eff}	3.046	3.23 ± 0.13 (3.18946)	3.046	3.28 ± 0.12 (3.28)
H_0 [km/s/Mpc]	68.80 ± 0.52 (68.50)	69.73 ± 0.82 (69.42)	68.19 ± 0.39 (68.22)	69.54 ± 0.80 (69.38)
CMB:lensing χ^2	8.83	8.81	8.52	9.17
CMB:TTTEEE χ^2	2350.05	2352	2348.86	2354.72
CMB:low l χ^2	22.04	21.48	22.83	21.93
CMB:lowE χ^2	395.88	397.82	399.52	396.51
Cooke χ^2	0.65	0.18	0.30	0.0037
Aver χ^2	0.23	0.92	0.22	1.56
SH0ES χ^2	15.18	10.56	16.75	10.71
JLA Pantheon18 χ^2	1034.85	1034.74	1034.77	1034.77
BAO χ^2	5.35	5.41	5.24	5.32
prior χ^2	5.89	3.71	4.51	3.30
total χ^2	3838.95	3835.63	3841.52	3838.00

TABLE I: Constraints (68%) and best-fit values in parentheses on the main parameters based on CMB+BAO+Pantheon+R19+BBN. The values of χ^2 in the lower rows are for the best-fit points in each model.

B. Discussions

As is well known, an increase of N_{eff} affects the fit with the observations of light elements, because it contributes the cosmic expansion at the BBN epoch and alters the p/n ratio. This leads to an increase in both the helium mass fraction Y_P and deuterium abundance D/H. By increasing N_{eff} , the CMB fit simultaneously indicates a larger $\Omega_b h^2$ which reduces D/H. In total, the enhancement of D/H is suppressed. As a result, the χ^2 of Y_P observations

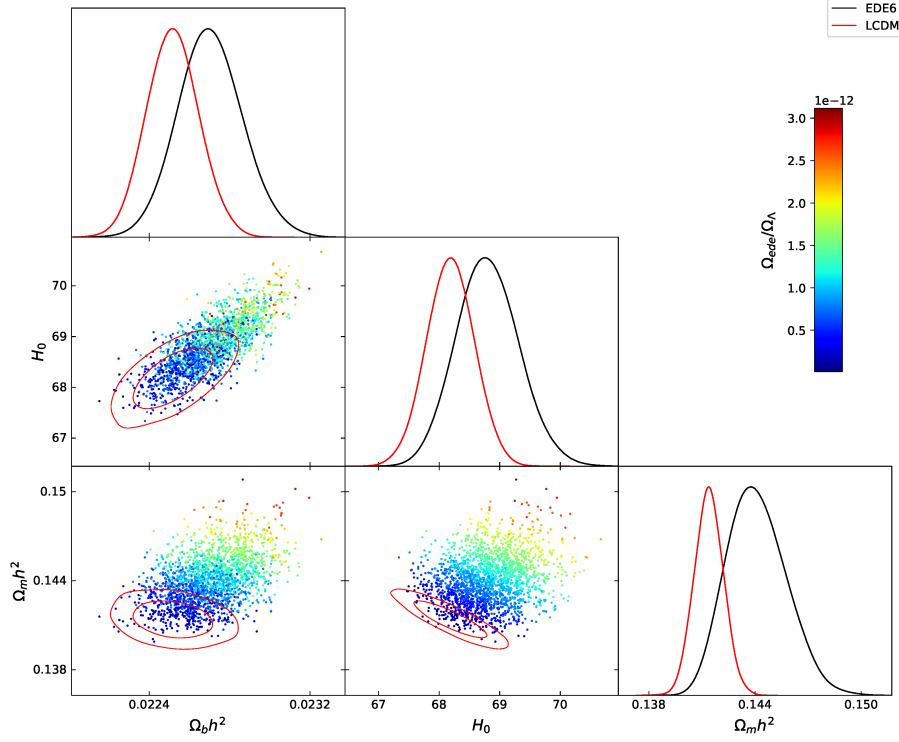


FIG. 3: Posterior and constraints on the EDE6 model. Red curves are for the Λ CDM model, for reference.

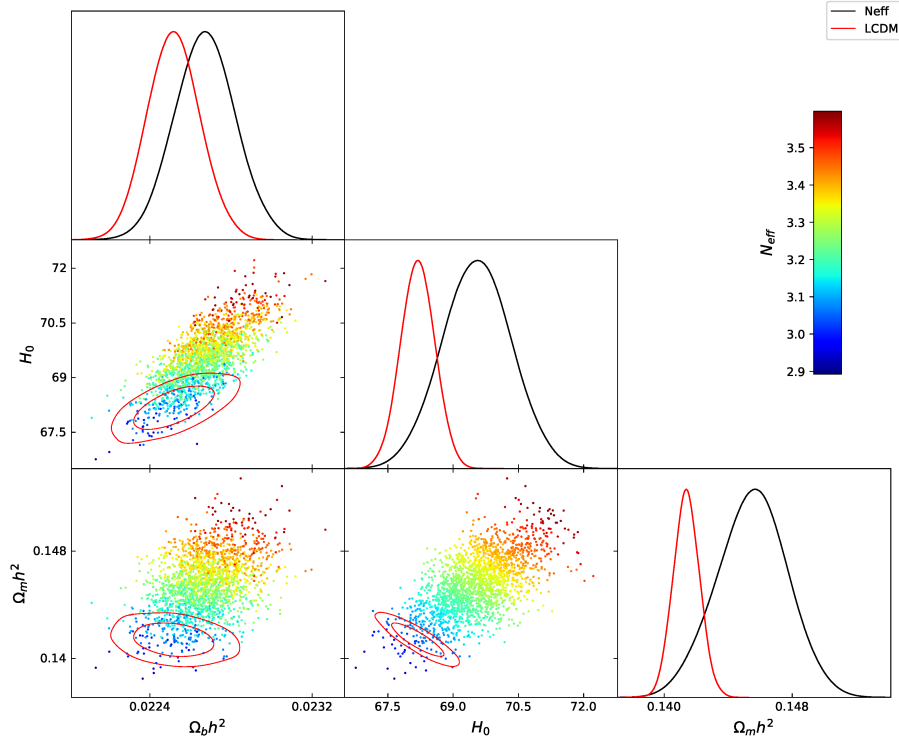


FIG. 4: Posterior and constraints on the N_{eff} model. Red curves are for the Λ CDM model, for reference.

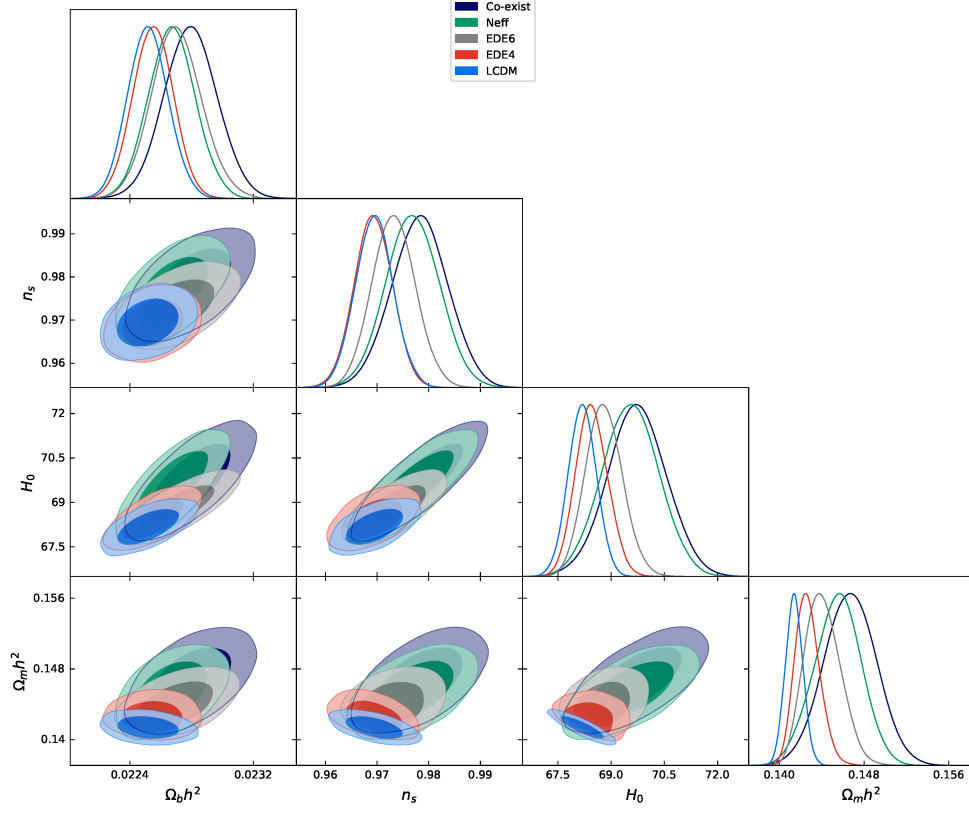


FIG. 5: Posterior and constraints of several models.

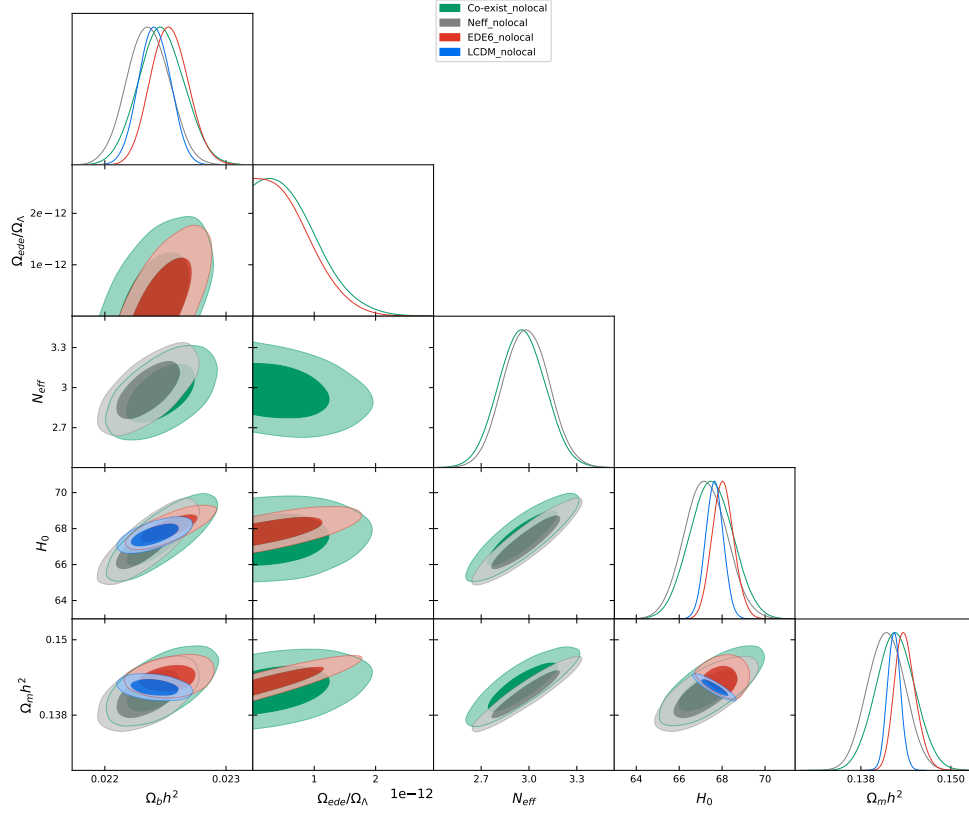


FIG. 6: Posterior and constraints of several models without including R19 data.

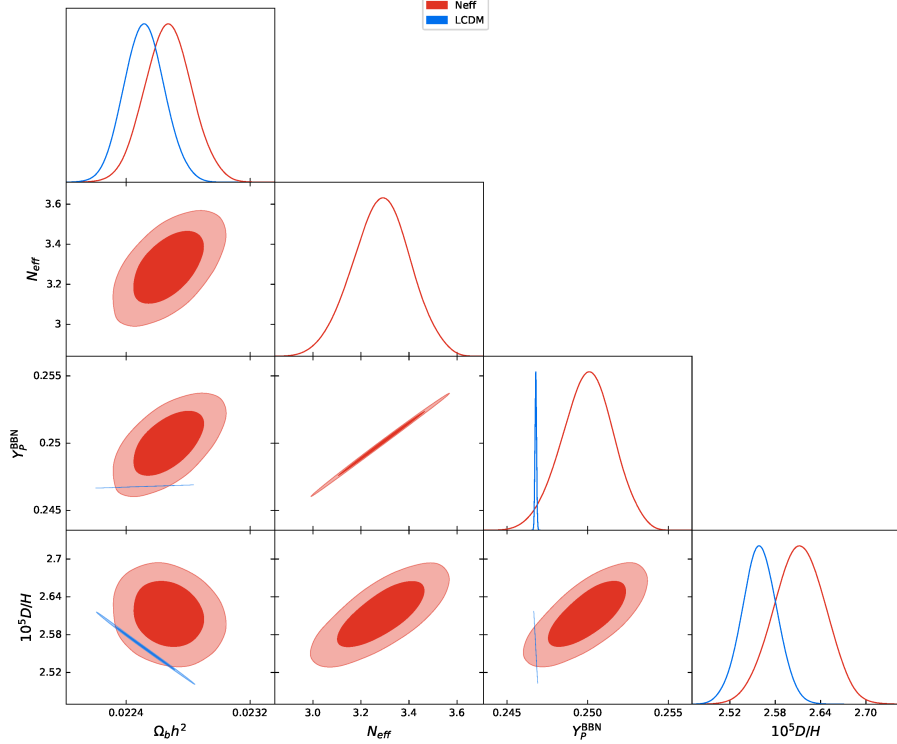


FIG. 7: Posterior and its BBN dependence in the N_{eff} model.

(χ^2_{Aver}) increases, while the χ^2 of D/H observations (χ^2_{Cooke}) increases a little. In fact, the value of χ^2_{Cooke} of the N_{eff} model is smaller than that in the ΛCDM model. This can be seen in Fig. 7 and Table I. On the other hand, in the EDE scenarios, increasing $\Omega_b h^2$ to adjust the CMB fit reduces the D/H abundance significantly. Thus, χ^2_{Aver} increases a little, while χ^2_{Cooke} increases. This can be seen in Fig. 8 and Table I. The tradeoff relation between the fit to the helium mass fraction Y_P and deuterium abundance D/H can be seen more clearly in Table I, where we compare it with the coexistence model.

The constraint on N_{eff} from BBN and BAO data only without including CMB or SH0SE data has been derived as $N_{\text{eff}} = 2.88 \pm 0.16$, which is less than 3 [50]. As is well known, a larger N_{eff} is disfavored by BBN. This is consistent with the results in Table I. What we additionally find is that the EDE models without ΔN_{eff} are also limited by BBN, because they predict too little D/H abundance by too large $\Omega_b h^2$.

In the literature on the new physics interpretation of the Hubble tension, data sets have not included BBN data. We have derived constraints from the data sets with and without BBN data for each model. As can be expected, data sets without BBN indicate larger values

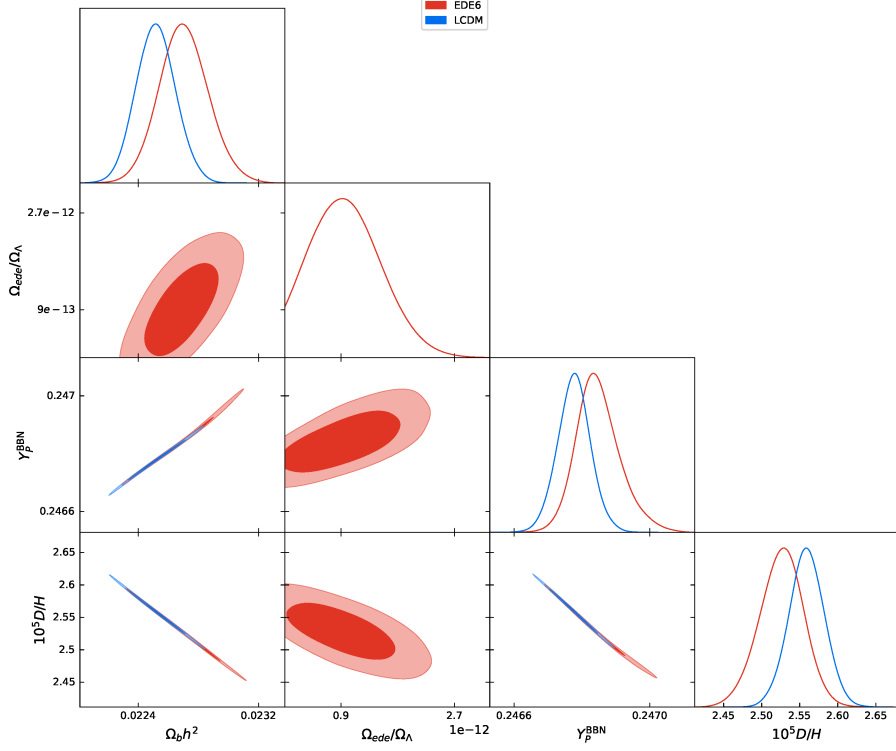


FIG. 8: Posterior and its BBN dependence in the EDE6 model.

of H_0 and N_{eff} . The magnitudes of the differences are shown in Fig. 9.

V. SUMMARY

A shorter sound horizon scale at the recombination epoch, arising from introducing extra energy components such as extra radiation or EDE is a simple approach to resolving the so-called Hubble tension. However, then the compatibility with successful BBN would be a concern, because the extra radiation may contribute to the cosmic expansion or the inferred baryon asymmetry would be different from that in the Λ CDM. We have compared the EDE models, N_{eff} model, and a coexistence model, paying attention to the fit to BBN. In fact, the EDE models are also subject to the BBN constraints by increasing the order-unity χ^2 as in the N_{eff} model. Our main results are summarized in Fig. 5 and Table I. By comparing the posteriors based on the CMB+BAO+Pantheon+R19 combined data, both the N_{eff} and a coexistence models indicate the largest H_0 between all of the models studied. H_0 can be as large as 70.5 km/s/Mpc within 1σ only for the coexistence model. The goodness of the fits for the models in terms of χ^2 are also listed in Table I. The fitting is good in the order

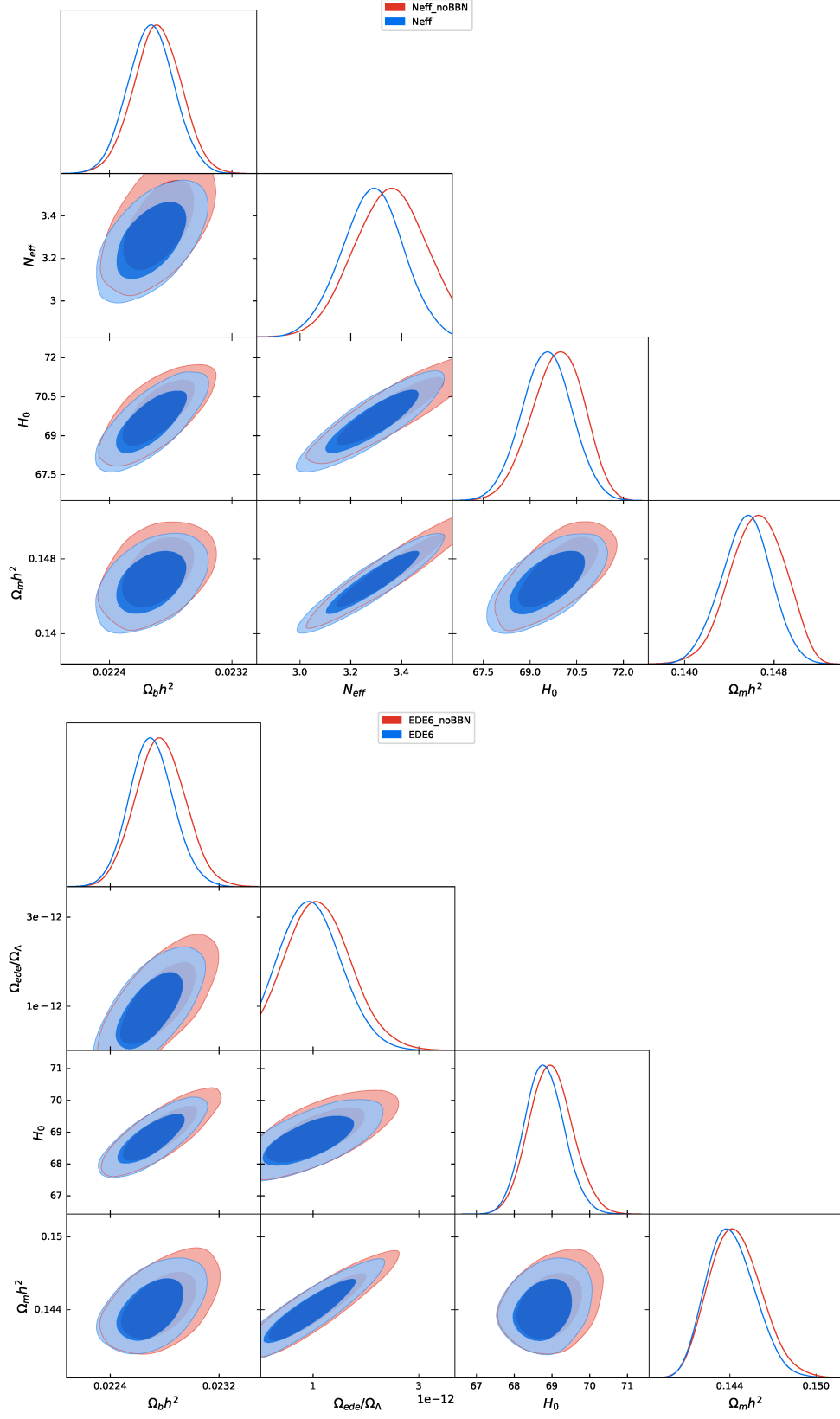


FIG. 9: Comparison of constraints based on data sets with and without BBN for the N_{eff} (upper) and EDE6 (lower) models.

of the $N_{\text{eff}}+\text{EDE6}$, N_{eff} , and EDE6 models and the ΛCDM . The difference of the best-fit H_0 values between the $N_{\text{eff}}+\text{EDE6}$ and N_{eff} models is tiny, while the χ^2 difference is about 2.4. The extra radiation seems to be more effective at causing a large H_0 than the EDE model. Thus, the N_{eff} model is a much simpler and better model than the EDE models.

We also examined the data sets dependence, whether we include BBN or not. The difference on N_{eff} in the N_{eff} model is only about 0.06 in its mean value, however, the including errors indicate

$$3.22 < N_{\text{eff}} < 3.49 \text{ (68\%)} \quad \text{for} \quad (\text{CMB} + \text{BAO} + \text{Pantheon} + \text{R19}), \quad (14)$$

$$3.16 < N_{\text{eff}} < 3.40 \text{ (68\%)} \quad \text{for} \quad (\text{CMB} + \text{BAO} + \text{Pantheon} + \text{R19} + \text{BBN}), \quad (15)$$

and there is almost 0.1 difference in the upper. By comparing this with Eq. (1), we can see the impact of the R19 data compared to the R18 data. For EDE models, if we include the BBN data, a smaller H_0 and smaller EDE energy density are preferred.

Acknowledgments

We would like to thank T. Sekiguchi for kind correspondences concerning the use of CosmoMC. This work is supported in part by the Japan Society for the Promotion of Science (JSPS) KAKENHI Grants Nos. 19K03860, 19H05091, and 19K03865 (O.S.).

-
- [1] N. Aghanim *et al.* (Planck Collaboration), *Astron. Astrophys.* **641**, A6 (2020).
 - [2] A. G. Riess *et al.*, *Astrophys. J.* **855**, 136 (2018).
 - [3] A. G. Riess, S. Casertano, W. Yuan, L. M. Macri and D. Scolnic, *Astrophys. J.* **876**, 85 (2019).
 - [4] K. C. Wong *et al.*, *Mon. Not. R. Astron. Soc.* **498**, 1420 (2020).
 - [5] G. Efstathiou, *Mon. Not. R. Astron. Soc.* **440**, 1138 (2014).
 - [6] W. L. Freedman, *Nat. Astron.* **1**, 0121 (2017).
 - [7] M. Rameez and S. Sarkar, [arXiv:1911.06456 [astro-ph.CO]].
 - [8] M. M. Ivanov, Y. Ali-Haïçemoud, and J. Lesgourgues, *Phys. Rev. D* **102**, 063515 (2020).
 - [9] J. L. Bernal, L. Verde and A. G. Riess, *J. Cosmol. Astropart. Phys.* **10** (2016) 019.
 - [10] K. Aylor, M. Joy, L. Knox, M. Millea, S. Raghunathan and W. L. K. Wu, *Astrophys. J.* **874**, 4 (2019).

- [11] F. D’Eramo, R. Z. Ferreira, A. Notari and J. L. Bernal, *J. Cosmol. Astropart. Phys.* **11** (2018) 014.
- [12] M. Escudero, D. Hooper, G. Krnjaic and M. Pierre, *J. High Energy. Phys.* **03** (2019) 071.
- [13] M. Escudero and S. J. Witte, *Eur. Phys. J. C* **80**, 294 (2020).
- [14] N. Okada and O. Seto, *Phys. Rev. D* **101**, 023522 (2020).
- [15] V. Poulin, K. K. Boddy, S. Bird and M. Kamionkowski, *Phys. Rev. D* **97** 123504 (2018).
- [16] V. Poulin, T. L. Smith, D. Grin, T. Karwal and M. Kamionkowski, *Phys. Rev. D* **98**, 083525 (2018).
- [17] V. Poulin, T. L. Smith, T. Karwal and M. Kamionkowski, *Phys. Rev. Lett.* **122**, 221301 (2019).
- [18] P. Agrawal, F. Y. Cyr-Racine, D. Pinner and L. Randall, [arXiv:1904.01016].
- [19] S. Alexander and E. McDonough, *Phys. Lett. B* **797**, 134830 (2019).
- [20] M. X. Lin, G. Benevento, W. Hu and M. Raveri, *Phys. Rev. D* **100**, 063542 (2019).
- [21] T. L. Smith, V. Poulin and M. A. Amin, *Phys. Rev. D* **101**, 063523 (2020).
- [22] K. V. Berghaus and T. Karwal, *Phys. Rev. D* **101**, 083537 (2020).
- [23] J. Sakstein and M. Trodden, *Phys. Rev. Lett.* **124**, 161301 (2020).
- [24] A. Chudaykin, D. Gorbunov and N. Nedelko, *J. Cosmol. Astropart. Phys.* **08** (2020) 013.
- [25] M. Braglia, W. T. Emond, F. Finelli, A. E. Gumrukcuoglu and K. Koyama, *Phys. Rev. D* **102**, 083513 (2020).
- [26] F. Niedermann and M. S. Sloth, *Phys. Rev. D* **102**, 063527 (2020).
- [27] M. Gonzalez, M. P. Hertzberg and F. Rompineve, *J. Cosmol. Astropart. Phys.* **10** (2020) 028.
- [28] M. X. Lin, W. Hu and M. Raveri, *Phys. Rev. D* **102**, 123523 (2020).
- [29] R. Murgia, G. F. Abellio and V. Poulin, *Phys. Rev. D* **103**, 063502 (2021).
- [30] A. Chudaykin, D. Gorbunov and N. Nedelko, *Phys. Rev. D* **103**, 043529 (2021).
- [31] L. Yin, [arXiv:2012.13917].
- [32] W. Hu and S. Dodelson, *Ann. Rev. Astron. Astrophys.* **40**, 171 (2002).
- [33] L. Knox and M. Millea, *Phys. Rev. D* **101**, 043533 (2020).
- [34] T. Sekiguchi and T. Takahashi, *Phys. Rev. D* **103**, 083507 (2021).
- [35] T. Sekiguchi and T. Takahashi, *Phys. Rev. D* **103**, 083516 (2021).
- [36] J. C. Hill, E. McDonough, M. W. Toomey and S. Alexander, *Phys. Rev. D* **102**, 043507 (2020).
- [37] M. M. Ivanov, E. McDonough, J. C. Hill, M. Simonović, M. W. Toomey, S. Alexander and

- M. Zaldarriaga, Phys. Rev. D **102**, 103502 (2020).
- [38] A. Cuceu, J. Farr, P. Lemos and A. Font-Ribera, J. Cosmol. Astropart. Phys. 10 (2019) 044.
 - [39] N. Schiöeneberg, J. Lesgourgues and D. C. Hooper, J. Cosmol. Astropart. Phys. 10 (2019) 029.
 - [40] E. J. Copeland, M. Sami and S. Tsujikawa, Int. J. Mod. Phys. D **15**, 1753 (2006).
 - [41] A. Lewis and S. Bridle, Phys. Rev. D **66**, 103511 (2002).
 - [42] O. Pisanti, A. Cirillo, S. Esposito, F. Iocco, G. Mangano, G. Miele and P. D. Serpico, Comput. Phys. Commun. **178**, 956 (2008)
 - [43] N. Aghanim *et al.* (Planck Collaboration), Astron. Astrophys. **641**, A8 (2020).
 - [44] F. Beutler, C. Blake, M. Colless, D. H. Jones, L. Staveley-Smith, L. Campbell, Q. Parker, W. Saunders and F. Watson, Mon. Not. R. Astron. Soc. **416**, 3017 (2011).
 - [45] A. J. Ross, L. Samushia, C. Howlett, W. J. Percival, A. Burden and M. Manera, Mon. Not. R. Astron. Soc. **449**, 835 (2015).
 - [46] S. Alam *et al.* (BOSS Collaboration), Mon. Not. R. Astron. Soc. **470**, 2617 (2017).
 - [47] D. M. Scolnic, D. O. Jones, A. Rest, Y. C. Pan, R. Chornock, R. J. Foley, M. E. Huber, R. Kessler, G. Narayan, A. G. Riess *et al.*, Astrophys. J. **859**, 101 (2018).
 - [48] E. Aver, K. A. Olive and E. D. Skillman, J. Cosmol. Astropart. Phys. 07 (2015) 011.
 - [49] R. J. Cooke, M. Pettini and C. C. Steidel, Astrophys. J. **855**, 102 (2018).
 - [50] R. H. Cyburt, B. D. Fields, K. A. Olive and T. H. Yeh, Rev. Mod. Phys. **88**, 015004 (2016).